SUPPLEMENTARY MATERIAL
Collective state transitions of exciton-polaritons loaded into a periodic potential

K. Winkler,[1] O. A. Egorov,[2] I. G. Savenko,[3,4,5] X. Ma,[2] E. Estrecho,[5] T. Gao,[5] S. Müller,[1] M. Kamp,[1] T. C. H. Liew,[6] E. A. Ostrovskaya,[5] S. Höfling,[1,7] and C. Schneider[1]

[1] *Technische Physik, Wilhelm-Conrad-Röntgen-Research Center for Complex Material Systems, Universität Würzburg, Am Hubland, D-97074 Würzburg, Germany*
[2] *Institute of Condensed Matter Theory and Solid State Optics, Abbe Center of Photonics, Friedrich-Schiller-Universität Jena, Max-Wien-Platz 1, 07743 Jena, Germany*
[3] *National Research University of Information Technologies, Mechanics and Optics (ITMO University), Saint-Petersburg 197101, Russia*
[4] *COMP Centre of Excellence at the Department of Applied Physics, P.O. Box 11000, FI-00076 Aalto, Finland*
[5] *Nonlinear Physics Centre, Research School of Physics and Engineering, The Australian National University, Canberra ACT 2601, Australia*
[6] *Division of Physics and Applied Physics, Nanyang Technological University 637371, Singapore*
[7] *SUPA, School of Physics and Astronomy, University of St Andrews, St Andrews KY16 9SS, United Kingdom*

Sample

The MBE-grown layered structure [see Fig. 1(a) and (b) in main text] of the microcavity consists of an AlAs-$\lambda/2$-cavity surrounded by 37 (32) bottom (top) AlGaAs/AlAs DBR mirror pairs while the active media comprises two stacks of 7 nm GaAs quantum wells distributed at the optical antinodes inside the cavity layer and at the first DBR interface. By patterning the 10 nm thick GaAs-layer on top of the cavity layer in an etch-and-overgrowth step, we introduce an attractive photonic potential with a height-difference of about 5 nm which amounts to about 5 meV. A one-dimensional periodic array of 40 circular mesas with 2 µm diameter and the period of $a = 3$ µm is depicted in main text Fig. 1(b). Because of the deep confinement, a gap between the ground and the first excited Bloch band evolves as large as 2.3 meV. More details on the process can be found in [1].

Condensation in the one dimensional periodic potential

Once the condensation threshold is crossed (at ~ 1 mW), and in agreement with previous experiments carried out in significantly shallower potentials [2], a polariton condensate forms in the band gap. The phenomenon of polariton condensation is accompanied by a strong nonlinear increase of the emitted luminescence intensity, manifested by a distinct s-shape in the input-output characteristics and strong drop in the linewidth (Fig. S1(a-c)).

Numerical modelling below and above threshold

The experimental observations of the polariton spectra for moderate pumping rates below and above the condensation threshold can be accurately modelled using a nonequilibrium Gross-Pitaevskii approach with additional stochastic terms [3] (see Eqs. (1-2) and related discussions in the main text). In particular, below the condensation threshold, up to three Bloch bands are visible in the spectrum of the lower polariton, as shown in Fig. S2(a). In order to suppress the radiation from the planar background outside the mesas we plotted the spectra recorded along the line connecting the trap's centers (i.e. for $y = 0$). It should be noted that due to a stochastic nature of the fluctuations in the model a particular attention has to be paid to an adequate resolution of the signal on a noisy background. An adapted version of Monte Carlo approach [3] was used to analyze the momentum-frequency distribution of the exciton-polaritons. In order to accumulate the necessary statistic we performed the long-term calculations covering the condensate dynamics over $20ns$. During these calculations a sequence of spatial-temporal Fourier-spectra recorded after every $100ps$ has been prepared. Then an subsequent averaging over the ensemble of these preliminary profiles gives an eventual momentum-frequency distribution of the exciton-polariton.

When excited by a narrow pump focused on a potential minimum (a trap site), the condensed state of exciton-polaritons forms in the gap, as demonstrated in Fig. 2 of the main text. Moreover, for a sufficiently narrow pump beam driving mostly one site of the lattice, the emission from the edge of the Brillouin zone ($k_{||} = \pm\pi/a$) survives against the relaxation to the ground state ($k_{||} = 0$) in a wide interval of pump powers exceeding up to five times

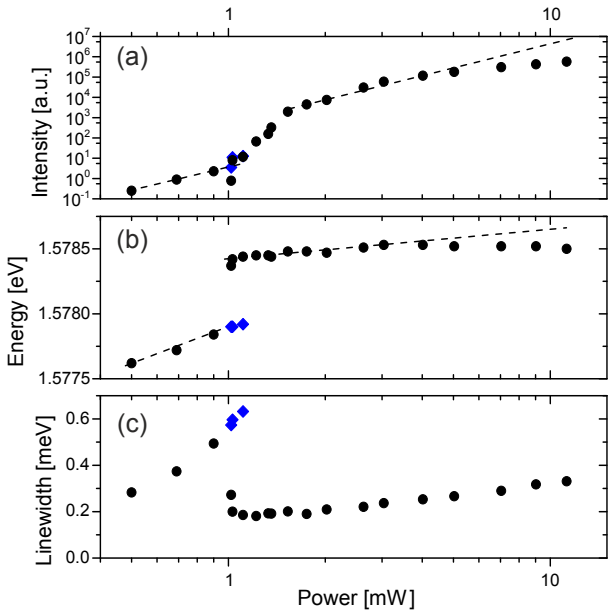

FIG. S1: (a-c) Analysis of intensity, energy and linewidth from a cut through the far field emission (corresponding to Fig. 2 in the main text) where the maxima appear above condensation threshold near the edges of the first Brillouin zone, namely at $k_{||} = 0.94\ \mu\text{m}^{-1}$. At the threshold region, ~ 1 mW, two peaks of the signal correspond to the uncondensed background (blue diamonds) and blueshifted condensate (black dots). Dashed lines are plotted as a guide to the eye.

the threshold value [see Figs. S2(b,c,d)]. At even stronger pumps [see Fig. S2(e)] the model ceases to be adequate since acoustic phonons-mediated energy scattering can not be neglected anymore (see the main text and discussions accompanying the Fig. 3). Numerical simulations confirm that the condensate bifurcates from the upper edges of the band and, thus, inherits the characteristic π-phase shift between two neighbouring sites, as shown in the real-space profiles of a single Monte Carlo realization of the polariton density and phase in Figs. S2(f,g).

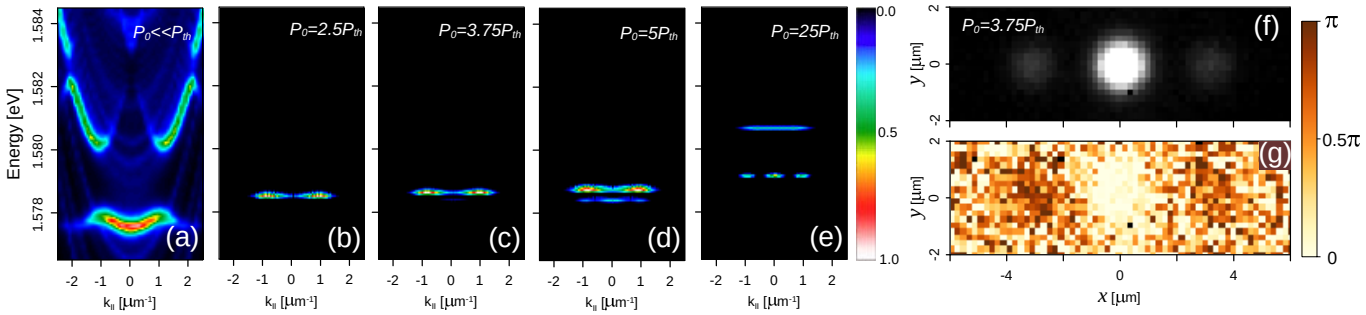

FIG. S2: (a) Polariton population (microcavity emission intensity) of different energy states below condensation threshold, $P_0 = 5\ \mu\text{m}^{-2}\text{ps}^{-1}$ ($P_{th} \approx 16\ \mu\text{m}^{-2}\text{ps}^{-1}$), calculated for a line connecting centers of the trapping potentials, $y = 0$. (b,c,d,e) Polariton condensate populations for various pump rates above the threshold, $P_0 > P_{th}$, for $P_0 = 40\ \mu\text{m}^{-2}\text{ps}^{-1}$, $P_0 = 60\ \mu\text{m}^{-2}\text{ps}^{-1}$, $P_0 = 80\ \mu\text{m}^{-2}\text{ps}^{-1}$ and $P_0 = 400\ \mu\text{m}^{-2}\text{ps}^{-1}$, respectively. (f,g) Snapshot of a single Monte Carlo realization of the intensity (f) and phase (g) profiles of the polaritons in the real space for $P_0 = 60\ \mu\text{m}^{-2}\text{ps}^{-1}$.

On-site vs. off-site loading: formation and stability of gap states.

The numerically modelled excitation spectra qualitatively reproduce the features of the on-site and off-site excitation with a tightly focused pump spot, see Fig. S3. On-site excitation with a pump beam centered on an individual mesa in the array (i.e., on one of the potential minima), leads to formation of an on-site gap state with a single prominent density peak in real space and two emission peaks near the edges of the Brillouin zone in momentum space. This

behaviour is extremely robust in the wide range of the pump powers, as discussed in the main text. Off-site excitation (pump laser focused on a barrier between two mesas), produces a prominent off-site gap state with the bulk of the emission in the momentum space centered near zero in-plane momentum and two density peaks in real space.

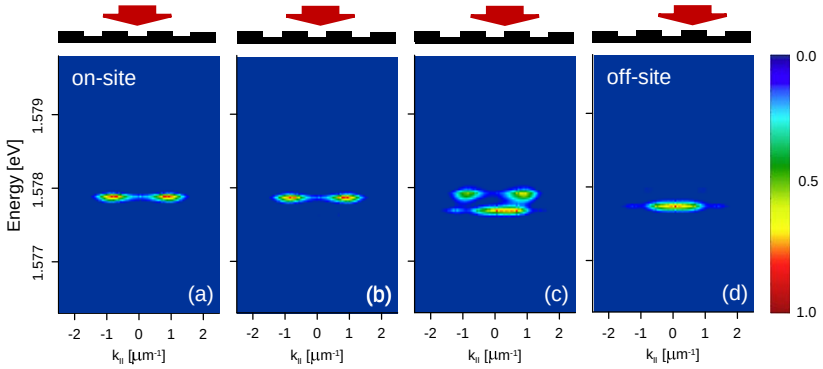

FIG. S3: Numerically calculated emission spectra for different positions of the excitation beam. (a) The case of "on-site" excitation, with the pump beam focused on the mesa. (b) The pump spot is shifted from the mesa's center at $\Delta x = 0.5\mu$m. (c) the pump spot is on the edge of the mesa, $\Delta x = 1.0\mu$m (d) The case of "off-site" excitation, i.e. the pump beam is focused between two mesas corresponding to a potential maximum, $\Delta x = 1.5\mu$m. The pump rate is above condensation threshold, $P_0 = 40\ \mu\text{m}^{-2}\text{ps}^{-1}$.

Precise control over the excitation of the on-site and off-site state by the respective positioning of the pump beam is a strong evidence for enhanced stability of the gap states in our tight-trapping potential, in contrast to more shallow lattices [4]. Indeed, it is well known that the on-site and off-site gap states in photonic lattices have very different stability properties [5], and both of these states become unstable deeper in the spectral gap. Similar behaviour is expected of polaritonic gap states. Indeed, excitation of an *off-site* gap state with an *on-site* pumping geometry observed in a shallow lattice [4] points towards instability of an on-site state for the moderate pump powers above threshold. In contrast, the tight-trapping lattice in our experiments supports stable formation of an *on-site* gap state triggered by an *on-site* excitation [as shown in Figs. 3 in the main text and S3(a)] for a wide range of pump powers [see Fig. S2(b-d)].

Controlled loading into a ground Bloch state.

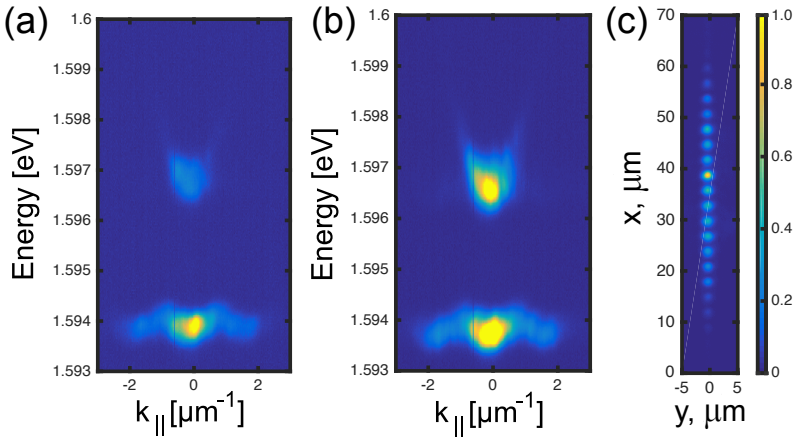

FIG. S4: (a,b) Experimentally measured microcavity emission spectra for an elliptical excitation beam with a high aspect ratio matched to the mesa array. The pump power is (a) $P = 5.48$ mW and (b) $P = 7.59$ mW. (c) Real space image of the condensate corresponding to the spectrum shown in (a).

As noted in the main text, controlled loading into a ground state of the lattice band-gap spectrum can be achieved by appropriate shaping of the pump beam. The experimental results for condensate excitation with a highly elongated

elliptical pump spot are demonstrated in Fig. S4. As can clearly be seen from the cavity emission spectrum above threshold Fig. S4(a), the polaritons are efficiently loaded into the ground band, with the high proportion of population in the Bloch state with $k_{||} = 0$ and characteristic multi-peak structure in the real space profile seen in Fig. S4(c). The width of the beam in the direction orthogonal to the array (~ 4 μm) is well matched to the mesa size, therefore the emission from the planar region is minimised. The absence of a strongly spatially localized potential due to the interaction with reservoir polaritons results in a suppressed blueshift of the condensed state compared to the gap state in Fig. 2 of the main text. In line with our observations for a strongly focused pump spot, at even higher pump powers, phonon-mediated redshift becomes prominent, while condensation at $k_{||} = 0$ prevails [see Fig. S4(b)].

[1] K. Winkler, J. Fischer, A. Schade, M. Amthor, R. Dall, J. Geßler, M. Emmerling, E.A. Ostrovskaya, M. Kamp, C. Schneider, and S. Höfling, New J. Phys. **17**, 023001 (2015).
[2] C. W. Lai, N. Y. Kim, S. Utsunomiya, G. Roumpos, H. Deng, M. D. Fraser, T. Byrnes, P. Recher, N. Kumada, T. Fujisawa, and Y. Yamamoto, Nature, **450**, 529 (2007).
[3] M. Wouters and V. Savona, Phys. Rev. B, **79**, 165302 (2009).
[4] D. Tanese, H. Flayac, D. Solnyshkov, A. Amo, A. Lemaitre, E. Galopin, R. Braive, P. Senellart, I. Sagenes, G. Malpuech, and J. Bloch, Nature Comm., **4**, 1749 (2013).
[5] A.A. Sukhorukov and Yu. S. Kivshar, Opt. Lett. **28**, 2345 (2003).